6

An Experimental and Numerical Study on the Compressible Laminar Flow Control

Shigeo Yoshida, Kinya Nakano and Nobuaki Shiozawa
Fuji Heavy Industries, Ltd.

ABSTRACT

Supersonic wind tunnel tests and numerical analyses were carried out on the boundary layer stability. Wind tunnel tests were performed on a swept wing model. Boundary layer transition locations were detected at various angles of attack and extensions of laminar flow regions by boundary layer suction were also observed. Consequently, the validity of supersonic laminar flow control was suggested.

And a boundary layer stability analyses code was developed, based on the linear stability theory, and its validity was confirmed for 2-dimensional boundary layers. Then one of the wind tunnel test cases was analyzed, and characteristics of disturbances were clarified.

NOMENCLATURE

C:chord length

$-C_Q$:suction mass flow rate

$[(-\rho V)_{wall}/(\rho U)_0]$

M:Mach Number

Q:non-dimensional mean flow quantities

q':perturbated quantities from the mean flow

R_C:Reynolds number on the chord length

R_{TR}:transition Reynolds number

R_x:Reynolds number based on x

$R\delta^*$:boundary layer Reynolds number on the displacement thickness

U,V,W:velocity component in x,y,z coordinate system

x,z,y:choordinates normal and parallel to the leading edge, and upper-wise

α:angle of attack

α, β:disturbance wave numbers(real parts) and amplification rates(negative imaginal parts), in x and z direction

$\alpha\delta^*$:non-dimensional wave number

$-\sigma$:local amplification rate of wavepacket

δ^*:boundary layer displacement thickness

Λ:sweep angle

ϕ:disturbance amplification functions

ψ:angle between inviscid flow velocity vector and wave number direction

ψ:$\cos^{-1}(|\psi|)$

ω:disturbance frequency

1.INTRODUCTION

Drag reduction at cruise condition is one of the most important themes in developing Supersonic Transports(SST). Among several drag reduction techniques, the laminar flow control(LFC) is the most promising one, because of its skin friction reduction benefit, as is mentioned in Ref.1. For its practical application, it is necessary to establish design tools and to validate its effectiveness. In general, accurate transition prediction is critical in designing and analyzing laminal flow wings. In cases of highly swept wings, like those of the SST, cross-flow(C-F) instability plays an important role in boundary layer transition phenomena, in addition to the Tollmien-Schlichting(T-S) instability. And to realize laminar flow wings, it is necessary to suppress such 3-dimensional instabilities. Hence, our objective is to reveal the characteristics of supresonic boundary layer transitions and the effectiveness of LFC for SST wings.

In this study, we focused on transitions caused by T-S and C-F instabilities, and aimed to accumulate 3-dimensional supersonic LFC wind tunnel test data and testing techniques, and establish numerical tools to predict effects of 3-dimensional supersonic LFC.

In this paper, we refer to the results of wind tunnel tests in section-2, numerical analyses in section-3, and conclusions in section-4.

2.WIND TUNNEL TEST

WIND TUNNEL TEST OVERVIEW

We carried out wind tunnel tests in the Fuji Heavy Industries 2ft×2ft high speed wind tunnel. The test model was installed as shown in Fig.1 in the test section. The model is a non-tapered swept wing which has a 240mmC NACA64A008 airfoil section in the direction normal to the leading edge. Its upper surface between 2.5%C and 30%C is interchangeable with a perforated panel which has 0.1mmϕ holes distributed at 1.0mm pitch. Pressure distribution, transition locations, and suction mass flow were measured during wind tunnel run time, where transition locations were detected by the visualization technique using liquid crystals. Test conditions are shown as follows.

- Mach number(M)=2
- sweep angle(Λ)=45° (supersonic leading edge)
  65° (subsonic leading edge)
- angle of attack(α)=-4° ~8°
- Reynolds number(R_C)=4.4×10^6(Λ=45°)
  7.4×10^6(Λ=65°)
- suction mass flow rate(-C_Q)=0(solid)
  0.001(perforated)

TEST RESULTS

The pressure distributions that were measured in the wind tunnel test are shown in Fig.2, and transition locations are also shown in Fig.3. Both results, without boundary layer suction, show that laminar regions extended as angles of attack increased, unless leading edge separation vortex caused the transition. It's known that cross-flow instability is dominant in accelerated regions on deeply swept wings. The pressure gradients, in the forward regions shown in Fig.2, got smaller as angles of attack increased. Consequently, cross-flow instability was suppressed as angles of attack increased.

Furthermore, the effect of boundary layer suction were observed in cases of Λ=45° . Transition

Reynolds numbers were increased by about 1 million; consequently, decrease in skin frictions are suggested. In cases of $\Lambda=65^\circ$, extensions of laminar boundary layer s were not observed.

3.NUMERICAL ANALYSIS

PROBLEM FORMULATION

In this study, we aimed to predict boundary layer transitions by the N-factor method, which is also available for supersonic LFC wings. Hence, we have developed a 3-dimensional compressible boundary layer stability analysis code, based on linear stability theory.

The stability equations are derived from non-dimensional NS equations. Each flow variable consists of two terms. One represents the stable flow variables and the other represents the time dependent term.

$$Q(x,y,z,t) = Qs(x,y,z) + q'(x,y,z,t) \tag{1}$$

When we discuss the spatial propagating wavy disturbance, it is often expressed in the manner of a wavy function as follows:

$$q' = \phi(y) \cdot \exp[i(\alpha x + \beta z - \omega t)] \tag{2}$$

where α and β are complex, and ϕ is amplitudes at neutral stability points. And the disturbance equations are written in the vector notation form.

$$d\phi_i / dy = \alpha_{ij} \cdot \phi_j \tag{3}$$

where αij is an 8 × 8 matrix whose elements were determined corresponding to α, β and boundary layer profiles. The disturbance equations and boundary conditions form an eigenvalue problem.

$$F(\alpha,\beta;\omega) = 0 + 0i \tag{4}$$

In 2-dimensional analyses(i.e.β =0+0i), to analyze the boundary layer stability corresponds to solving the eigenvalue problem. However, in 3-dimensional analyses, one more condition is required to solve the eigen value problem. In this study, a wave number direction($\alpha_r \beta_r$) is also given as the condition, and the wavepacket assumption gives local amplifications($-\sigma$) and integrated amplification rate(N) as follows:

$$-\sigma = -\alpha_i + \beta_i (\partial\alpha_r / \partial_r\beta) \tag{5}$$

$$N = \int_{x0}^{x} (-\sigma) dx \tag{6}$$

NUMERICAL PROCEDURE

The prediction procedure consists of 4 phases.

1)inviscid analysis[2)]

2)boundary layer analysis[3)]

3)stability analysis

4)transition prediction(N-factor method)

CODE VALIDATION

To validate the analysis procedure, comparisons were made between present analyses and other analyses or experiments.

Fig.4 shows the comparison of the neutral stability profile for the Blasius' boundary layer between the one calculated in this study and Schlichting's[4]. Fig.5 shows growths of disturbances on a NACA0012 airfoil at zero incidence. Each line shows the disturbance growth of a certain frequency and the transition point was predicted as the intersection of the envelop of growth lines and transition criterion(N=9), and △ indicates the test result[5]. Furthermore, Fig.6 shows comparison of the transition Reynolds numbers of flat plate boundary layers with experiments[6]. Each analysis(Fig.4-6) shows good agreement with other analyses and experiments.

NUMERICAL ANALYSIS

Boundary layer stability analyses were carried out on the test case, M=2, $\Lambda=45^\circ$, $\alpha=0^\circ$, $R_C=4.4\times10^6$, $-C_Q=0$(solid surface). Fig.7 shows the neutral stability profile. Fig.7 shows that cross-flow instability is dominant in the region, which is consistent with the wind tunnel test results. Fig.8 shows the growth if there are disturbances. It shows that each disturbance gradually changes its direction from cross-flow instability to T-S.

4.CONCLUSIONS

Through supersonic wind tunnel tests, useful transition data were obtained and the extension of laminar regions were also observed; consequently, the validity of supersonic LFC was suggested. In this study on the numerical analyses, the validity of our stability analysis procedure was confirmed in 2-dimensional boundary layers. Furthermore, boundary layer stability characteristics in the leading edge region were made clear in the series of wind tunnel tests.

REFERENCES

[1]Douglas Aircraft Company, "Study on High-Speed Civil Transports", NASA-CR-4235.

[2]Kamo. K., "Development of Three-Dimensional Compressible Navier-Stokes Analysis Code", 20th Conference on Fluid Dynamics, The Japan Society for Aeronautical and Space Science, and the Japan society for Fluid Dynamics, 1988.

[3]Kaups. T .and Cebeti. T., "Compressible Boundary Layer with Suction on Swept and Tapered Wings", Journal of Aircraft, Vol.14, No.7, Jul, 1977, pp.661-667.

[4]Schlichting. H., "Boundary-Layer Theory", 1979, p.139.

[5]Von Doenhoff. A.E., "Investigation of the Boundary-Layer about a Symmetrical Airfoil in a Wind Tunnel of Low Turbulence", Rept.L-507, 1940, NACA.

[6]Mack. L.M., "Linear Stability Theory and the Problem of Supersonic Boundary Layer Transition", AIAA Journal, Vol.13, No.3, Mar, 1975, pp.278-289.

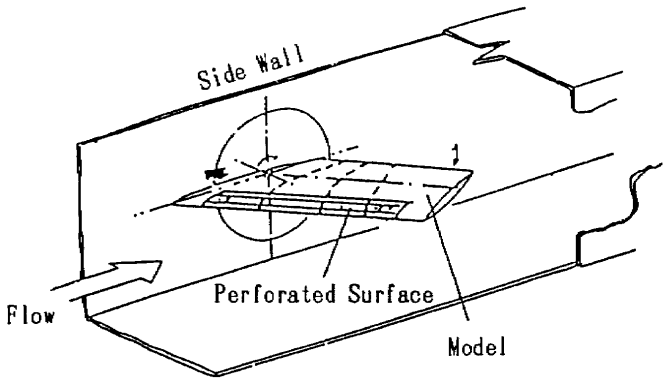

Fig. 1 Model Installation
in FHI High Speed Wind Tunnel

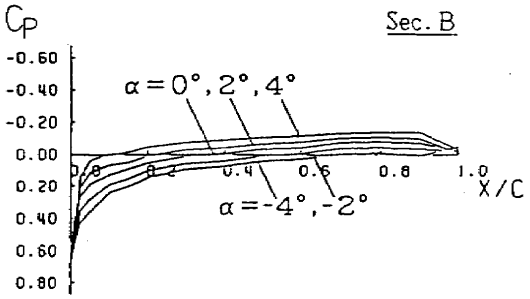

Fig. 2(a) Upper Surface Pressure Distribution
[Λ=45°, Solid]

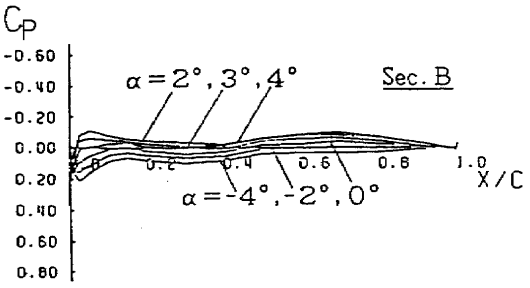

Fig. 2(b) Upper Surface Pressure Distribution
[Λ=65°, Solid]

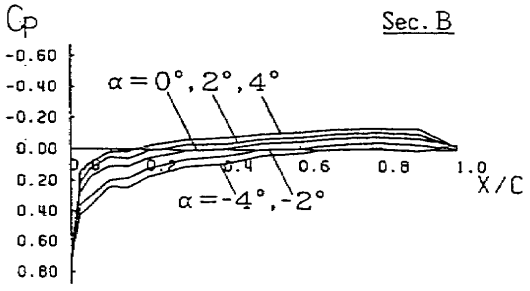

Fig. 2(c) Upper Surface Pressure Distribution
[Λ=45°, -C_Q=0.001]

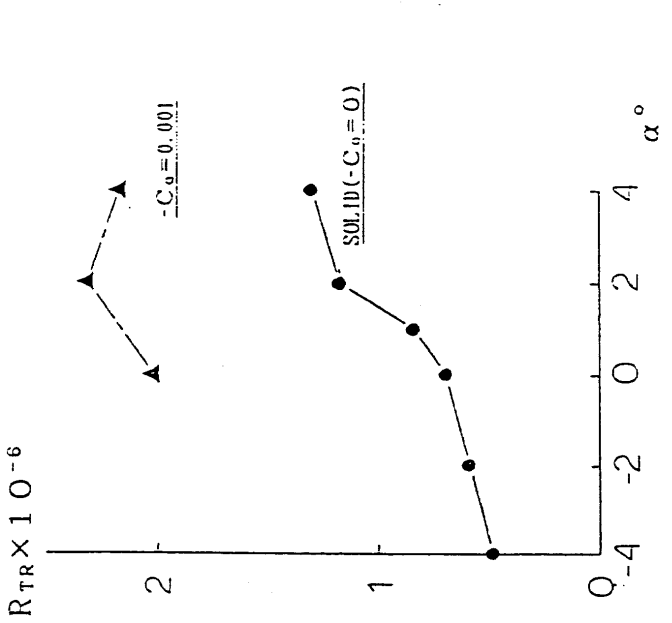

Fig. 3(b) Transition Reynolds Number [$\Lambda = 45°$]

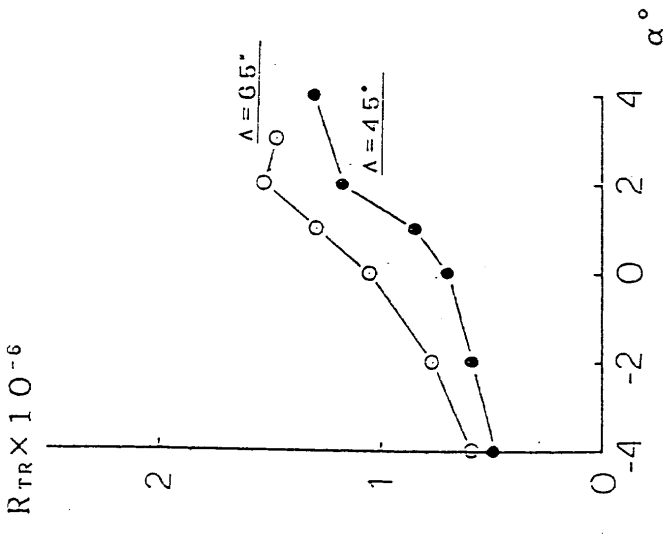

Fig. 3(a) Transition Reynolds Number [Solid]

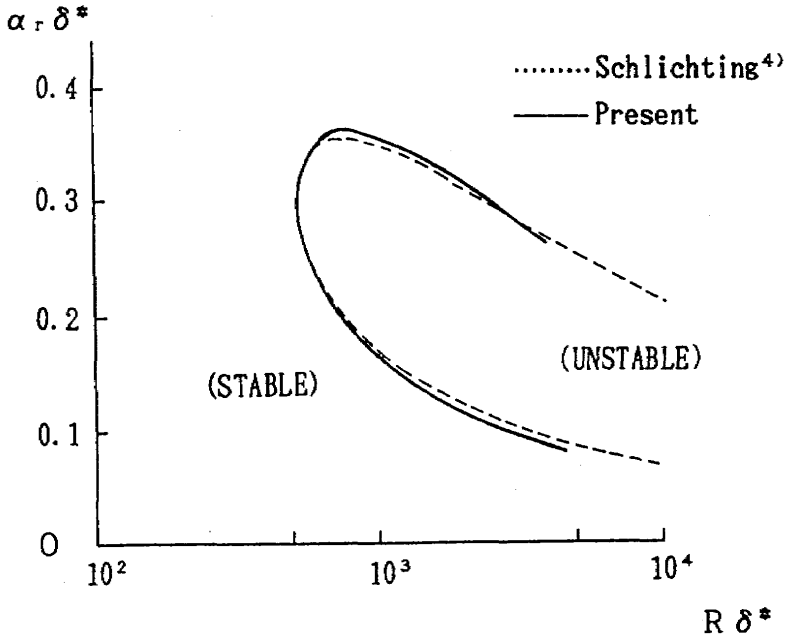

Fig. 4 Stability of Blasius Boundary Layer

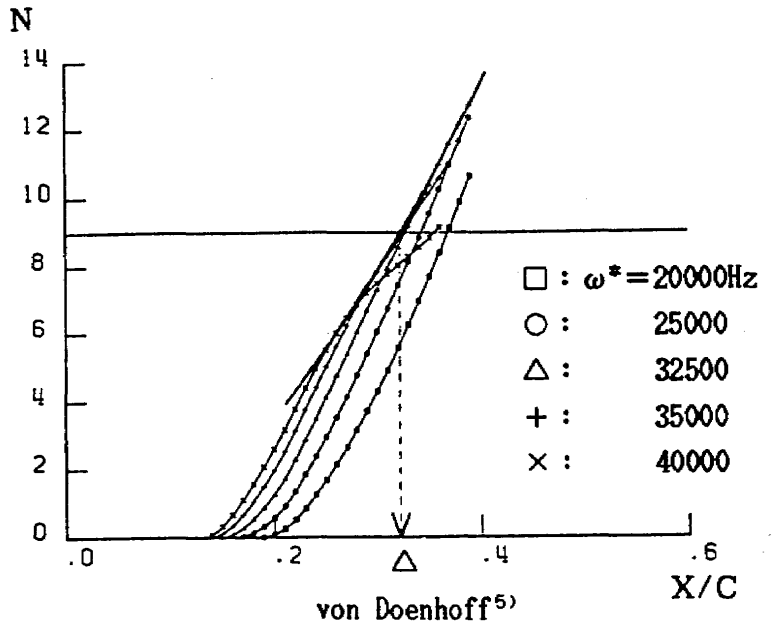

Fig. 5 Transition Location on NACA0012

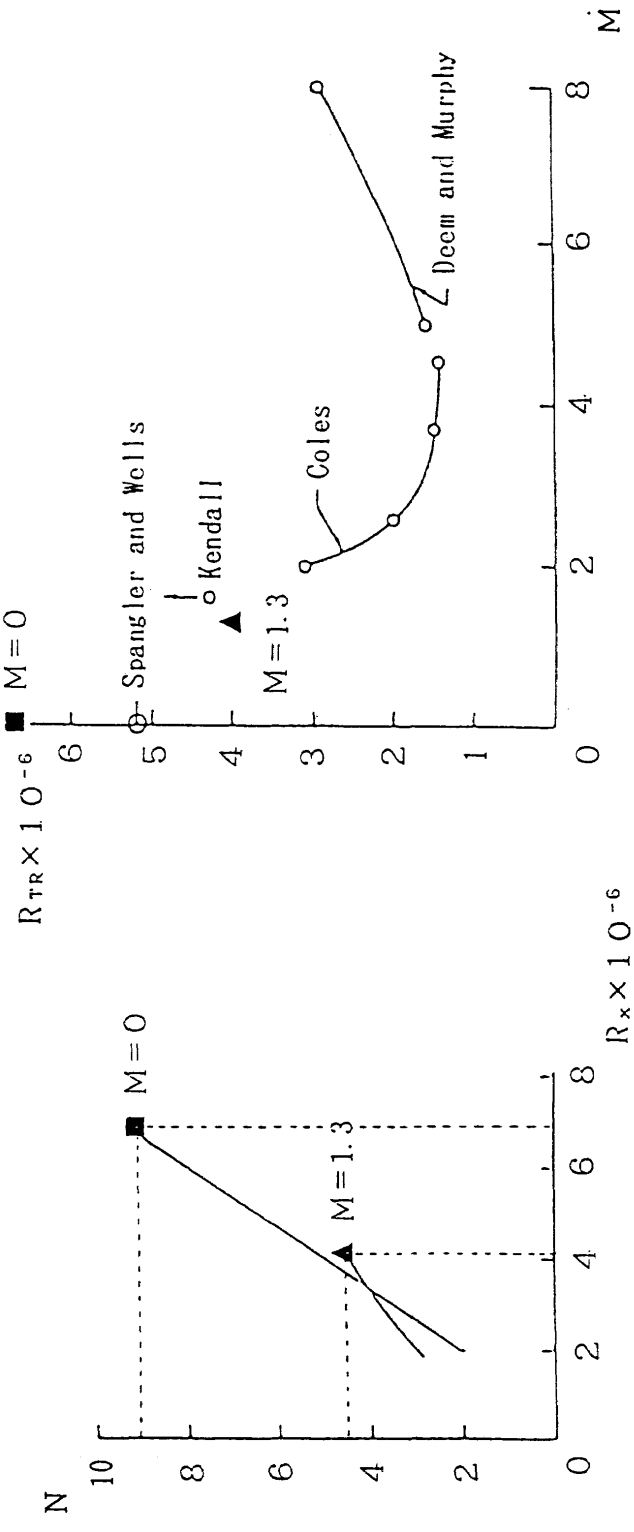

Fig. 6(a) Integrated Amplification Ratio and Transition Reynolds Number on Flat Plate

Fig. 6(b) Transition Reynolds Number on Flat Plate

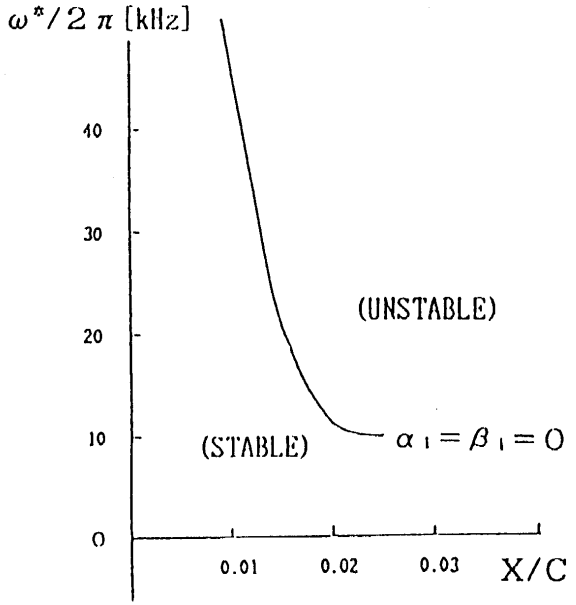

Fig. 7(a) Neutral Stability Profile on NACA64A008 Swept Wing [Amplification, M=2, Λ=45°, α=0°]

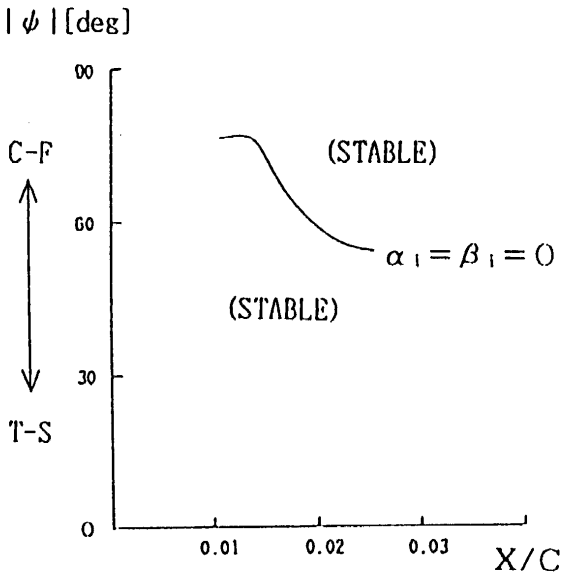

Fig. 7(b) Neutral Stability Profile on NACA64A008 Swept Wing [Wave Number Direction, M=2, Λ=45°, α=0°]

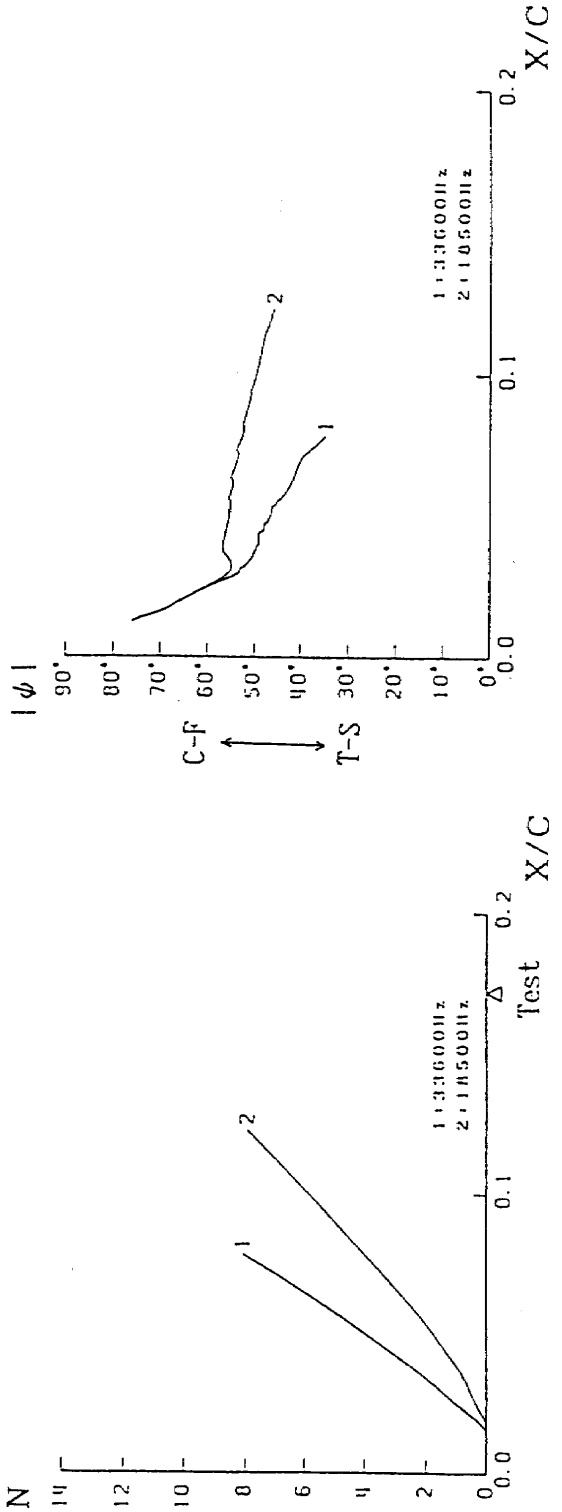

Fig. 8(a) Growth of Disturbance on NACA64A008 Swept Wing [Amplification, M=2, Λ=45°, α=0°]

Fig. 8(b) Growth of Disturbance on NACA64A008 Swept Wing [Wave Number Direction, M=2, Λ=45°, α=0°]